

This is an Open Access document downloaded from ORCA, Cardiff University's institutional repository: <https://orca.cardiff.ac.uk/id/eprint/73396/>

This is the author's version of a work that was submitted to / accepted for publication.

Citation for final published version:

Li, Y.-C., Cleall, P. J. , Wen, Y.-D., Chen, Y.-M. and Pan, Q. 2015. Stresses in soil-bentonite slurry trench cut-off walls. *Géotechnique* 65 (10) , pp. 843-850. 10.1680/jgeot.14.P.219

Publishers page: <http://dx.doi.org/10.1680/jgeot.14.P.219>

Please note:

Changes made as a result of publishing processes such as copy-editing, formatting and page numbers may not be reflected in this version. For the definitive version of this publication, please refer to the published source. You are advised to consult the publisher's version if you wish to cite this paper.

This version is being made available in accordance with publisher policies. See <http://orca.cf.ac.uk/policies.html> for usage policies. Copyright and moral rights for publications made available in ORCA are retained by the copyright holders.



1
2
3
4
5
6 **Stresses in Soil-Bentonite Slurry Trench Cutoff Walls**
7
8
9

10
11 **Authors:** Yu-Chao Li* (BEng, PhD, Associate Professor);

12 Peter John Cleall† (BEng, PhD, Senior Lecturer);

13 Yi-Duo Wen* (BEng, MEng candidate);

14 Yun-Min Chen* (BEng, MSc, PhD, Professor);

15 Qian Pan* (BEng, PhD candidate).
16
17
18
19
20
21

22 *MOE Key Laboratory of Soft Soils and Geoenvironmental Engineering, Department of
23 Civil Engineering, Zhejiang University, Hangzhou 310058, China.

24 †Geoenvironmental Research Centre, Cardiff School of Engineering, Cardiff University,
25 Cardiff, CF24 3AA, Wales, UK.
26
27
28
29
30
31
32

33 **Submitting author:**

34 Name: Yu-Chao Li

35 Contact address: MOE Key Laboratory of Soft Soils and Geoenvironmental Engineering,
36 Department of Civil Engineering, Zhejiang University, Hangzhou 310058, China.
37
38

39 Telephone: +86-571-88208859
40

41 E-mail address: yuchao_li@hotmail.com.
42
43
44
45
46
47
48
49
50
51
52
53
54
55
56
57
58
59
60
61
62
63
64
65

1
2
3
4 **Abstract:** The long-term performance of soil-bentonite slurry trench cutoff walls is
5
6 highly dependent on the hydraulic conductivity of the soil-bentonite backfill, which
7
8 according to laboratory tests can decrease significantly as consolidation pressure
9
10 increases due to corresponding reductions in void ratio. Consequently a reliable estimate
11
12 of the hydraulic conductivity of backfill in the field requires proper calculation of
13
14 effective stresses. A model is proposed to predict the steady-state horizontal and vertical
15
16 effective stresses in the backfill after consolidation. The arching effect is considered via
17
18 force equilibrium, and the lateral squeezing effect of inward displacement of the trench
19
20 sidewalls is considered by assuming the cutoff wall is surrounded by soil which is
21
22 represented by a Winkler idealization. The proposed model is applied to model a soil-
23
24 bentonite slurry trench cutoff wall at Mayfield, New South Wales, Australia, and the
25
26 predicted stress profile is in good agreement with that calculated from cone penetration
27
28 tests data. Compared to those predicted by geostatics and other alternative models, the
29
30 proposed method offers a significant improvement in the prediction of stress in SB slurry
31
32 trench walls. The obtained stresses are then used to estimate the hydraulic conductivity
33
34 in the backfill. It is found that the hydraulic conductivity is relatively high in the shallow
35
36 region owing to the low state of effective stresses, which requires consideration in cutoff
37
38 wall design, and decreases slightly with the depth in the deeper region. Finally a
39
40 parametric study identifies the side wall friction and the modulus of horizontal subgrade
41
42 reaction of surrounding soil as having the most significant impact on the estimated
43
44 stresses.
45
46
47
48
49
50
51
52
53

54
55
56
57 **Keywords:** cut-off walls and barriers; permeability; stress analysis; trenches
58
59
60
61
62

1
2
3
4 **1. Introduction**
5
6
7

8
9 Soil-bentonite (SB) slurry trench cutoff walls are commonly constructed to contain
10 subsurface contamination as part of a remediation strategy for contaminated sites.
11
12 Typically a trench is excavated in the ground, with the trench being filled with slurry to
13
14 maintain the trench stability. Then SB backfill is placed into the trench displacing the
15
16 slurry to form a vertical barrier. The primary design criterion in SB cutoff wall design is
17
18 an achievement of a low-permeability backfill barrier in the trench. Many laboratory
19
20 tests show that hydraulic conductivity of SB decreases significantly as consolidation
21
22 pressure increases due to corresponding reductions in void ratio (Evans 1994; Filz et al.,
23
24 2001; Yeo et al., 2005). Accordingly, the *in-situ* stress state of SB backfills has a
25
26 considerable effect on the hydraulic barrier performance of cutoff walls and subsequently
27
28 a reliable estimate of the hydraulic conductivity of backfills in the field depends on the
29
30 proper calculation of *in-situ* effective stress (Evans et al. 1995). The stress-state in the
31
32 SB also has a critical influence on resistance to chemical attack and hydraulic fracturing
33
34 of backfill (Filz 1996).
35
36
37
38
39
40
41
42
43
44

45 Early field and laboratory studies (McCandless & Bodocsi 1987; Bennert et al., 2005)
46
47 indicate that the effective stress state in SB cutoff walls is much lower than that predicted
48
49 by a geostatic approach where only the effective weight of the overlying backfill is
50
51 considered. This finding has also been confirmed by various theoretical models (Evans et
52
53 al., 1995; Filz, 1996; Ruffing et al., 2010). If the confining stress used in the laboratory
54
55 tests is based on the vertical geostatic stress distribution the hydraulic conductivity of SB
56
57
58
59
60
61
62
63
64
65

1
2
3
4 backfill may be significantly underestimated, leading to a non-conservative design.
5
6 Crucially, current design procedures of SB cutoff walls do not include consideration of
7
8 the state of stress in backfill, and research efforts on SB cutoff walls has been largely
9
10 limited to laboratory investigations, despite the need for an understanding of how the
11
12 stress develops *in situ* (National Research Council, 2007; Ruffing et al., 2012).
13
14
15
16
17
18
19

20 The SB backfill consolidates under a vertical load from the weight of overlying backfill
21
22 and a lateral squeezing load induced by the inward displacement of trench sidewalls. A
23
24 closed-form solution based on an arching mechanism approach, conventionally applied to
25
26 buried pipelines, was proposed by Evans et al. (1995) to calculate the steady-state vertical
27
28 effective stresses in backfill of SB cutoff walls. This solution considers backfill sidewall
29
30 friction, which reduces vertical stress in the backfill to magnitudes below that of the
31
32 overburden pressure. However, in this approach the trench sidewalls are assumed to be
33
34 rigid, which may result in an underestimation of the horizontal effective stress by
35
36 ignoring strength gain in the backfill realized by inward movement of the trench
37
38 sidewalls (Ruffing et al., 2010). An alternative “lateral squeezing” model had been
39
40 proposed by Filz (1996) primarily accounting for the lateral squeezing mechanism due to
41
42 the trench sidewalls’ movement towards the trench centerline after backfill placement.
43
44 Consistencies of lateral force and displacement at the interface between the backfill and
45
46 the surrounding soil are considered. However, this model assumes that the sidewall
47
48 frictional forces are capable of reducing the vertical stresses in the backfills (caused by
49
50 overlying backfills) to negligible values, and so the obtained stresses are not dependent
51
52 on the backfill overburden pressure. As noted by Filz (1996) this assumption is not valid
53
54
55
56
57
58
59
60
61
62
63
64
65

1
2
3
4 for wide and shallow trenches. The lateral squeezing model was modified by [Ruffing et](#)
5 [al. \(2010\)](#) to incorporate consideration of the stress-dependent nature of SB backfill's
6
7 compressibility. The primary limitations of the lateral squeezing models ([Filz, 1996;](#)
8
9 [Ruffing et al., 2010](#)) are firstly that the ground adjacent to the trench is assumed to be in
10
11 an at-rest condition prior to backfill compression, which may lead to errors in prediction
12
13 of the steady-state stresses, and secondly that the relationship between lateral earth
14
15 pressure (or lateral earth pressure coefficient) and trench sidewall movement, which the
16
17 lateral squeezing models require, is not well established in the literature.
18
19
20
21
22
23
24
25

26 A model is proposed in this paper to predict the steady-state effective stresses in backfill
27
28 of SB slurry trench cutoff walls. It combines the ideas of two existing models ([Evans et](#)
29 [al., 1995; Filz, 1996](#)) considering both the arching and lateral squeezing mechanisms.
30
31 The proposed model is then applied to model the stress distribution in a SB cutoff wall at
32
33 Mayfield, New South Wales, Australia. The stress profile obtained by the proposed
34
35 model is compared with that calculated from results of cone penetration tests given by
36
37 [Ruffing et al. \(2015\)](#) as well as those predicted by geostatics, the arching model and the
38
39 modified lateral squeezing (MLS) model. The hydraulic conductivity of the backfill with
40
41 depth is estimated based on the obtained stresses. Finally, a parametric study is carried
42
43 out to investigate the impacts of backfill/surrounding soil properties on the effective
44
45 stresses in backfill.
46
47
48
49
50
51

52 53 54 55 56 57 58 **2. Theory** 59 60 61 62 63 64 65

1
2
3
4
5
6
7 A SB slurry trench cutoff wall, whose width and depth are B and L , respectively, within a
8
9 soil medium is considered in this paper (see Fig. 1). It is assumed that the groundwater
10
11 level is at the surface and that the SB backfill is fully saturated after placement (Evans et
12
13 al., 1995; Filz, 1996; Ruffing et al., 2010). The longitudinal strain of backfill after the
14
15 placement is assumed to be zero and so the geometry of the problem can be considered to
16
17 be plane-strain. For simplicity, in the subsequent text the horizontal direction refers to
18
19 the transverse direction. A two-dimensional coordinate system, whose positive direction
20
21 is downward, is adopted, and the ground surface is chosen as the origin of z .
22
23
24
25
26
27

28
29 At the end of backfill placement, the self-weight of the SB is assumed to be fully carried
30
31 by the pore water, that is, the pore water pressure $u = \gamma_w z + \gamma'_{sb} z$ in the backfill at the
32
33 depth z (see Table 1), where γ_w is the unit weight of water and γ'_{sb} is the buoyant unit
34
35 weight of SB backfill; the horizontal and vertical effective stresses in the backfill
36
37 $\sigma'_h = \sigma'_v = 0$; and the excess pore water pressure $u_e = \gamma'_{sb} z$. When the backfill is
38
39 consolidated, u_e becomes zero; the pore water pressure decreases to hydrostatic pressure,
40
41 that is, $u = \gamma_w z$; and the steady-state effective stresses σ'_h and σ'_v require determination.
42
43
44
45
46
47
48
49

50 The horizontal strain increment between the times of completion of backfill placement
51
52 and backfill consolidation can be written as (Timoshenko, 1970),
53

$$54 \Delta \varepsilon_h = \frac{1 - \mu^2}{E} \left(\Delta \sigma'_h - \frac{\mu}{1 - \mu} \Delta \sigma'_v \right) = \frac{1 - \mu^2}{E} \left(\sigma'_h - \frac{\mu}{1 - \mu} \sigma'_v \right) \quad (1)$$

55
56
57
58
59
60
61
62
63
64
65

1
2
3
4 where $\Delta\varepsilon_h$, $\Delta\sigma'_h$ and $\Delta\sigma'_v$ are, respectively, the increments of horizontal strain,
5
6 horizontal effective stress and vertical effective stress in the backfill between the times of
7
8 completion of backfill placement and backfill consolidation; E and μ are the Young's
9
10 modulus and Poisson's ratio of backfill, respectively.
11
12
13
14

15
16
17 The hydraulic conductivity of the surrounding soil is commonly greater than that of the
18
19 SB backfill by at least one or two orders of magnitude. Consequently, the consolidation
20
21 of the surrounding soil mass is assumed to be finished instantaneously, and the horizontal
22
23 effective stress in the surrounding soil, $\sigma'_{h,s}$, can then be determined as follows,
24
25
26

$$\sigma'_{h,s} = \sigma_h - \gamma_w z \quad (2)$$

27
28 where σ_h is the horizontal total stress in backfill and its values at the end of backfill
29
30 placement and the time of backfill consolidation completion are given in Table 1.
31
32 According to the Winkler's idealization (Selvadurai, 1979), the surrounding soil is
33
34 assumed to be equivalent to an infinite number of independent elastic springs (see Fig. 1).
35
36 The deformation of the foundation at any point is directly proportional to the stress
37
38 applied at that point. So the horizontal deformation of the trench sidewall between the
39
40 time of SB backfilling completion and that of SB consolidation completion can be written
41
42 as follows using Equ. (2),
43
44
45
46
47
48
49

$$\Delta y = \frac{\Delta\sigma'_{h,s}}{k} = \frac{\gamma'_{sb} z - \sigma'_h}{k} \quad (3)$$

50
51 where Δy is the horizontal deformation of the trench side wall and $\Delta\sigma'_{h,s}$ is the
52
53 horizontal effective stress increment in the surrounding soil; and k is the modulus of
54
55
56
57
58
59
60
61
62
63
64
65

horizontal subgrade reaction of the surrounding soil. Using Equ. (3), the horizontal strain increment can also be written as

$$\Delta \varepsilon_h = \frac{2\Delta y}{B} = \frac{2}{Bk}(\gamma'_{sb} z - \sigma'_h) \quad (4)$$

The following relationship between σ'_v and σ'_h can be obtained by combining Eqs. (1) and (4):

$$\sigma'_v = D\sigma'_h - A\gamma'_{sb} z \quad (5)$$

where

$$A = \frac{2E}{\mu(1+\mu)Bk} \quad (6)$$

$$D = \frac{1-\mu}{\mu} + A \quad (7)$$

The vertical force equilibrium of a typical backfill element with a thickness dz (see Fig. 1) considering the “arching” effect (Handy, 1985) has the following expression, when the backfill is consolidated:

$$2\tau dz + (u + du)B + (\sigma'_v + d\sigma'_v)B = uB + \sigma'_v B + \gamma_{sb} B dz \quad (8)$$

where γ_{sb} is the unit weight of the SB backfill; $Bdu = B\gamma_w dz$; and τ is the sidewall frictional stress at the backfill-surrounding soil interface (Evans et al., 1995; Ruffing et al., 2010) and is assumed to follow the Mohr-Coulomb strength criterion as follows,

$$\tau = c'_{inter} + \sigma'_h \tan \phi'_{inter} \quad (9)$$

1
2
3
4 where c'_{inter} and ϕ'_{inter} are the cohesion and internal friction angle of the interface,
5
6
7 respectively, and they are assumed to have the following relationships with those of SB
8
9
10 backfill (Potyondy, 1961):

$$11 \quad c'_{\text{inter}} = c'_{\text{sb}} / R \quad (10)$$

$$12 \quad \tan \phi'_{\text{inter}} = \tan \phi'_{\text{sb}} / R \quad (11)$$

13
14
15 where c'_{sb} and ϕ'_{sb} are the cohesion and internal friction angle of the backfill,
16
17
18 respectively; and R is the shear strength reduction factor. Equ. (8) can be re-written using
19
20
21 as follows Eqs. (5), (9)-(11),
22
23

$$24 \quad \sigma'_h + \frac{BD}{2 \tan \phi'_{\text{inter}}} \frac{d\sigma'_h}{dz} - \frac{B\gamma'_{\text{sb}}}{2 \tan \phi'_{\text{inter}}} \left(1+A - \frac{2c'_{\text{inter}}}{B\gamma'_{\text{sb}}} \right) = 0 \quad (12)$$

25
26
27
28
29
30 Equ. (12) is the governing equation in terms of the steady-state σ'_h . It is assumed that
31
32
33 there is no surcharge load and so the steady-state horizontal effective stress at the top
34
35
36 boundary of the cutoff wall can be written as

$$37 \quad \sigma'_h = 0 \quad \text{at } z = 0 \quad (13)$$

38
39
40 Given σ'_h is known, σ'_v can be obtained using Equ. (5). The modulus of horizontal
41
42
43 subgrade reaction k for soils has the following general form (Bowles, 1996):
44
45

$$46 \quad k = A_s + B_s z^n \quad (14)$$

47
48
49 where A_s is constant; B_s is coefficient for depth variation; and n is exponent to give k the
50
51
52 best fit. This non-linear relationship can be reduced to a linear form, which is commonly
53
54
55 used in foundation engineering (Das, 1998), by taking a value of $n=1$ yielding:

$$56 \quad k = n_h z \quad (15)$$

57
58
59 where n_h is the constant of modulus of horizontal subgrade reaction.
60
61
62
63
64
65

Equ. (12) can then be solved via a numerical method, with the finite element method used in this paper. It is noted that Equ. (12) has the following closed-form solution if k is assumed to be constant in depth:

$$\sigma'_h = \frac{B\gamma'_{sb}}{2 \tan \phi'_{inter}} \left(1 + A - \frac{2c'_{inter}}{B\gamma'_{sb}} \right) \left[1 - \exp \left(- \frac{2 \tan \phi'_{inter}}{BD} z \right) \right] \quad (16)$$

The squeezing effect due to inward displacements of trench sidewalls is considered in Equ. (16) via the coefficients A and D (as defined in Eqs. (6) and (7)). This equation can be compared to the following solution of the arching model (Ruffing et al., 2010), which assumes the trench sidewalls are rigid,

$$\sigma'_h = K_{ob} \sigma'_v = \frac{B\gamma'_{sb}}{2 \tan \phi'_{inter}} \left(1 - \frac{2c'_{inter}}{B\gamma'_{sb}} \right) \left[1 - \exp \left(- \frac{2K_{ob} \tan \phi'_{inter}}{B} z \right) \right] \quad (17)$$

where K_{ob} is the at-rest earth pressure coefficient of the backfill.

3. Validation

In order to assess the validity of the proposed model it has been applied to one of the only experimental datasets related to SB slurry trench cutoff walls where estimates of *in-situ* stress conditions are available. This case study relates to a SB cut-off wall constructed at the Mayfield site which is an area of land approximately 155 ha on the south bank of the Hunter River near Newcastle in New South Wales, Australia. Full details can be found in Jones et al. (2007); Ryan & Spaulding (2008) and Ruffing et al. (2015).

1
2
3
4 The most polluted part of the site, known as Area 1, was previously occupied by coke
5 ovens, gas holders and other processes associated with steelmaking over a period of
6 approximately 85 years. The geoenvironmental testing of samples from test pits showed
7 that this site was high polluted by polycyclic aromatic hydrocarbons, Benzo(a)pyrene,
8 Chromium and Lead. A SB slurry trench cutoff wall was designed and installed through
9 a sand layer (which varied from 30 m to 50 m thick) to divert up gradient groundwater
10 flows away from Area 1 and to stop the movement of contaminations towards the river.
11 It is 1,510 m long, 0.8 m wide and has depths ranging from 25 m to 49 m. The excavated
12 trench was backfilled with a SB mixture consisting of a blend of excavated soil, imported
13 clay and bentonite slurry. A minimum fines (passing 75µm sieve) content of 20% in the
14 backfill blend was checked daily with a target of achieving a permeability specification
15 of less than 1×10^{-8} m/s (Jones et al 2007).
16
17
18
19
20
21
22
23
24
25
26
27
28
29
30
31
32
33
34
35

36 As part of the quality control program a series of cone penetration tests with pore
37 pressure readings (CPTu) was performed producing 24 CPTu profiles through the full
38 depth of the cutoff wall. In addition a vane test was performed to a depth of 18 m at one
39 of the cone locations. The effective cone resistance method was selected from five
40 potential methods (Powell & Lunne, 2005) by Ruffing et al. (2015) to predict the
41 undrained shear strength (S_u) vs. depth, that is,
42
43
44
45
46
47
48
49

$$S_u = \frac{q_t - u_2}{N_{ke}} \quad (18)$$

50
51 where u_2 is pore pressure from CPTu data; N_{ke} is the theoretical cone factor with a value
52 of $N_{ke}=11.5$ reported by Ruffing et al. (2015) based on the coupled CPTu and vane shear
53 data; finally q_t is the corrected tip resistance via the following equation:
54
55
56
57
58
59
60
61
62
63
64
65

1
2
3
4
5
6
7
8
9
10
11
12
13
14
15
16
17
18
19
20
21
22
23
24
25
26
27
28
29
30
31
32
33
34
35
36
37
38
39
40
41
42
43
44
45
46
47
48
49
50
51
52
53
54
55
56
57
58
59
60
61
62
63
64
65

$$q_t = q_c + (1-a)u_2 \quad (19)$$

where q_c is raw tip resistance; and a is area ratio (reported as 0.73 by [Ruffing et al. \(2015\)](#) for these tests).

The major principal effective stress σ'_0 in the SB cutoff wall for this project (see Fig. 2) was calculated by [Ruffing et al. \(2015\)](#) from average S_u vs. depth of all 24 CPTu data sets, using a S_u / σ'_0 ratio of 0.22. This ratio was selected by [Ruffing et al. \(2015\)](#) based on a review of available values for normally consolidated soils. It is noted that the values of cone resistance were deleted if they were significantly larger than the surrounding data points (>300-500 kPa), as they may be caused by pieces of gravel suspended in the backfill. It can be seen in Fig. 2 that the major principal stress at a depth greater than 5 m is significantly less than that predicted by geostatics. This is consistent with the findings of early field and laboratory studies ([McCandless & Bodocsi, 1987](#); [Bennert et al., 2005](#)).

[Ruffing et al. \(2015\)](#) assumed the horizontal effective stress was the major principal stress and controlled the backfill strength but recognized that the state of stress in SB slurry trench cutoff walls is not fully understood. As shown in Fig. 2, the horizontal effective stress predicted by [Ruffing et al. \(2015\)](#) using the arching model or the MLS model (with $K_{ob}=0.5$) is significantly less than the major principal stress calculated from the CPTu data. This is likely the result of only one of the arching and lateral squeezing effects being considered by each of these two models.

1
2
3
4 The proposed method is adopted to predict the effective stresses in the SB slurry trench
5
6 cutoff wall installed at Mayfield. The values used for the geometry and material
7
8 properties are listed in Table 2. The Poisson's ratio used for the backfill is based on data
9
10 reported by [Baxter \(2000\)](#) for soil-bentonite backfills. The linear relationship between k
11
12 and depth ([Das, 1998](#)) is used with the average value of n_h for submerged medium dense
13
14 sand and dense sand ([Das, 1998](#); [DHURDZP, 2014](#)) according to the geotechnical
15
16 condition of the site ([Jones et al., 2007](#)). The shear strength of the backfill-surrounding
17
18 soil interface is relatively low as a bentonite filter cake forms between backfill and
19
20 surrounding soil during the construction of slurry trench cutoff walls, according to the
21
22 findings of [Lam et al \(2014\)](#). Based on this, the shear strength reduction factor R is
23
24 selected from the range between 0.10 and 0.20 via calibration using the major principal
25
26 stress calculated from the CPTu data. It is recognized that direct measurement of R
27
28 would reduce uncertainty related to this parameter; such measurements could be obtained
29
30 following the approach reported by [Lam et al \(2014\)](#). The sensitivity of the model to this
31
32 parameter is explored in the subsequent parametric study. The obtained vertical effective
33
34 stress, which is greater than the horizontal one and assumed to be the major principal
35
36 stress following the discussion of [Ruffing et al. \(2015\)](#), by the proposed method is in
37
38 good agreement with that calculated from the CPTu data (see Fig. 2). Compared to those
39
40 predicted by the arching model and the MLS model, the proposed model offers a
41
42 significant improvement in the prediction of stress in SB slurry trench walls. This results
43
44 from the proposed method considering the combined effects of arching and lateral
45
46 squeezing.
47
48
49
50
51
52
53
54
55
56
57
58
59
60
61
62
63
64
65

The hydraulic conductivity of backfill (k_b) with depth can be estimated with the obtained stresses via consideration of changes in void ratio. Large strain consolidation models are available (e.g. [Fox et al. \(2014\)](#)) that relate the change in hydraulic conductivity to changes in void ratio through the compression curve; alternatively these relationships can be determined experimentally. As the relationship between the hydraulic conductivity and the effective consolidation stress is not available for the backfill material used in the Mayfield project, the following relationships for a sand-bentonite containing 5% dry bentonite tested by [Yeo et al. \(2005\)](#) are used to illustrate the potential impact:

$$e = 1.25 - 0.21 \log \left(\frac{\sigma' (\text{kPa})}{5} \right) \quad (20)$$

$$k_b (\text{cm/s}) = 1.5 \times 10^{-7} \times 10^{\frac{e-1.25}{0.22}} \quad (21)$$

where σ' is effective consolidation stress. As the consolidometer imposes one-dimensional loading conditions on the specimens the void ratio of the soil-bentonite is controlled by mean consolidation stress, rather than major principal consolidation stress ([Adams et al., 1997](#)). Consequently, the effective stresses obtained by the proposed model are converted to the equivalent vertical effective stress that would produce the same void ratio in one-dimensional compression condition following [Filz et al. \(2001\)](#):

$$\bar{\sigma}' = \frac{3\sigma'_{\text{mean}}}{1 + 2K_{\text{ob}}} \quad (22)$$

where $\bar{\sigma}'$ is the equivalent vertical effective stress; σ'_{mean} is the mean effective stress in backfill; and K_{ob} is assumed to be $\mu / (1 - \mu)$ for the consolidometer tests. $\bar{\sigma}'$ can be re-written as the following express for the plane-strain problem considered in this paper:

$$\bar{\sigma}' = (1 - \mu)(\sigma'_v + \sigma'_h) \quad (23)$$

1
2
3
4
5
6
7 Fig. 3 shows the estimated hydraulic conductivity profile based on the effective stresses
8
9 obtained by the proposed model. In the shallow region ($z \leq 2.5$ m), k_b is relatively high
10
11 owing to the low state of effective stresses (see Fig. 2); it then decreases with depth as
12
13 effective stresses increase. In the deep region ($z > 5.0$ m), the estimated hydraulic
14
15 conductivity decreases slightly with the depth as a result of the relatively constant value
16
17 of the mean effective stress, and reaches a value of $\sim 1 \times 10^{-10}$ m/s at the depth of 30 m.
18
19 According to the test results of [Yeo et al. \(2005\)](#), $k_b \leq 10^{-9}$ m/s can be achieved for the
20
21 backfill containing only low-plasticity clay and the backfill consisting of clean, coarse-
22
23 grained materials with a significant amount of dry bentonite if the effective consolidation
24
25 stress $\sigma' \geq 10$ kPa. Consequently the hydraulic conductivity specification can be
26
27 achieved at this site if the sand-bentonite reported by [Yeo et al. \(2005\)](#) is assumed to be
28
29 used. The estimated hydraulic conductivity profile based on the geostatic stress is also
30
31 shown in Fig. 3. It can be found that whilst the geostatic approach gives a good
32
33 prediction in the shallow region ($z < 5.0$ m), it underestimates the hydraulic conductivity in
34
35 the deep region ($z > 5.0$ m), which may lead to a non-conservative design.
36
37
38
39
40
41
42
43
44
45
46
47

48 **4. Parametric study**

49
50
51
52

53 In this section, the proposed model is applied to investigate the impacts of
54
55 backfill/surrounding soil properties on the steady-state effective stresses in backfill.
56
57
58
59
60
61
62
63
64
65

1
2
3
4 Finally a discussion on the closed-form solution to the case with a constant k assumption
5
6 is made.
7
8
9

10
11 The parameter values used to define trench geometry and material properties in the
12 following investigations are listed in Table 3. In the table the values ahead of the
13 brackets represent a base case scenario and those in the brackets define a range of values
14 used to investigate the impact of the corresponding parameter. For the base case scenario,
15 the width of the trench is 0.6 m; the depth of the trench is 30.0 m (the results obtained are
16 also applicable to scenarios where $L < 30$ m); the values for the properties of the SB
17 backfill are based on [Ruffing et al. \(2010\)](#); the constant of modulus of horizontal
18 subgrade reaction submerged medium sand ([Das, 1998](#)) is used for the surrounding soil
19 (that is, $n_h = 4.8 \text{ MN/m}^4$); and the value for the shear strength reduction factor for the
20 backfill-surrounding soil interface (that is, $R = 0.12$) is based on the Mayfield case
21 presented in the validation section.
22
23
24
25
26
27
28
29
30
31
32
33
34
35
36
37
38
39
40

41 The lateral squeezing effect of inward displacements of the trench sidewalls on the
42 backfill is investigated via consideration of various values of n_h , in particular values of
43 1.2 MN/m^4 , 4.8 MN/m^4 and 10.6 MN/m^4 , which correspond to submerged loose, medium
44 and dense sands, respectively ([Das, 1998](#)), are used. These values are based on those
45 recommended for the design of retaining structures for foundation excavations
46 ([DHURDZP, 2014](#)). As shown in Fig. 4(a) the horizontal effective stress, σ'_h , decreases
47 due to less lateral squeezing effect as n_h increases. The effective stresses for the scenario
48 in a dense sand formation are close to those for that in a medium sand formation, but they
49
50
51
52
53
54
55
56
57
58
59
60
61
62
63
64
65

are significantly different to those in a loose sand formation, which has a greater lateral squeezing force due to deformation of the sidewalls.

The vertical effective stress, σ'_v , predicted by the arching model (Ruffing et al., 2010), which assumes no lateral deformation of sidewalls, increases and tends towards

$$\frac{B\gamma'_{sb}}{2K_{ob} \tan \phi'_{inter}} \left(1 - \frac{2c'_{inter}}{B\gamma'_{sb}} \right)$$

as the depth increases (see Equ. (16)), that is, the weight of backfill tends to be taken by the sidewall friction with only a small increment in vertical effective stress with depth in the deeper regions. However, it is noted that, for the scenario in a loose sand formation, the vertical effective stress decreases as the depth increases when $z > 15$ m due to higher horizontal effective stress induced by the lateral squeezing effect, which is considered in the proposed method.

The constrained modulus of the SB backfill M is in the range between 500 kPa to 1600 kPa based on a series of one-dimensional consolidation test tests for sand-bentonite with dry bentonite contents of 4 and 5 % (Yeo et al., 2005) and for SB backfill collected from a cutoff wall site in eastern Pennsylvania (Ruffing et al., 2010). The Young's modulus E of the backfill has the following relationship with M , according to elasticity theory:

$$E = \frac{(1 + \mu)(1 - 2\mu)}{1 - \mu} M \quad (24)$$

Three cases with $E=312$ kPa, 654 kPa and 997 kPa are considered for $M=500$ kPa, 1050 kPa and 1600 kPa, respectively. As shown in Fig. 4(b), compared to the use of $E=654$ kPa, the relative differences in σ'_h and σ'_v by using $E=312$ kPa are 4.7% and 0.1% respectively, and are 4.4% and 0.3% respectively by using $E=997$ kPa, at $z=15$ m.

1
2
3
4 Consequently it can be concluded that, Young's modulus of SB backfill does not have a
5 major impact on the steady-state effective stresses in backfill and the use of a constant
6
7
8
9 Young's modulus will not lead to appreciable errors.

10
11
12
13
14 The arching effect due to the trench sidewall friction is highly dependent on the shear
15 strength reduction factor R , as shown in Fig. 4(c), which illustrates effective stress
16 profiles for three cases with varied values of R (specified based on the Newcastle case
17 modeled previously). The values of vertical effective stress for the cases with $R=0.2$, and
18
19
20
21
22
23
24
25
26
27
28
29
30
31
32
33
34
35
36
37
38
39
40
41
42
43
44
45
46
47
48
49
50
51
52
53
54
55
56
57
58
59
60
61
62
63
64
65
66
67
68
69
70
71
72
73
74
75
76
77
78
79
80
81
82
83
84
85
86
87
88
89
90
91
92
93
94
95
96
97
98
99
100
101
102
103
104
105
106
107
108
109
110
111
112
113
114
115
116
117
118
119
120
121
122
123
124
125
126
127
128
129
130
131
132
133
134
135
136
137
138
139
140
141
142
143
144
145
146
147
148
149
150
151
152
153
154
155
156
157
158
159
160
161
162
163
164
165
166
167
168
169
170
171
172
173
174
175
176
177
178
179
180
181
182
183
184
185
186
187
188
189
190
191
192
193
194
195
196
197
198
199
200
201
202
203
204
205
206
207
208
209
210
211
212
213
214
215
216
217
218
219
220
221
222
223
224
225
226
227
228
229
230
231
232
233
234
235
236
237
238
239
240
241
242
243
244
245
246
247
248
249
250
251
252
253
254
255
256
257
258
259
260
261
262
263
264
265
266
267
268
269
270
271
272
273
274
275
276
277
278
279
280
281
282
283
284
285
286
287
288
289
290
291
292
293
294
295
296
297
298
299
300
301
302
303
304
305
306
307
308
309
310
311
312
313
314
315
316
317
318
319
320
321
322
323
324
325
326
327
328
329
330
331
332
333
334
335
336
337
338
339
340
341
342
343
344
345
346
347
348
349
350
351
352
353
354
355
356
357
358
359
360
361
362
363
364
365
366
367
368
369
370
371
372
373
374
375
376
377
378
379
380
381
382
383
384
385
386
387
388
389
390
391
392
393
394
395
396
397
398
399
400
401
402
403
404
405
406
407
408
409
410
411
412
413
414
415
416
417
418
419
420
421
422
423
424
425
426
427
428
429
430
431
432
433
434
435
436
437
438
439
440
441
442
443
444
445
446
447
448
449
450
451
452
453
454
455
456
457
458
459
460
461
462
463
464
465
466
467
468
469
470
471
472
473
474
475
476
477
478
479
480
481
482
483
484
485
486
487
488
489
490
491
492
493
494
495
496
497
498
499
500
501
502
503
504
505
506
507
508
509
510
511
512
513
514
515
516
517
518
519
520
521
522
523
524
525
526
527
528
529
530
531
532
533
534
535
536
537
538
539
540
541
542
543
544
545
546
547
548
549
550
551
552
553
554
555
556
557
558
559
560
561
562
563
564
565
566
567
568
569
570
571
572
573
574
575
576
577
578
579
580
581
582
583
584
585
586
587
588
589
590
591
592
593
594
595
596
597
598
599
600
601
602
603
604
605
606
607
608
609
610
611
612
613
614
615
616
617
618
619
620
621
622
623
624
625
626
627
628
629
630
631
632
633
634
635
636
637
638
639
640
641
642
643
644
645
646
647
648
649
650
651
652
653
654
655
656
657
658
659
660
661
662
663
664
665
666
667
668
669
670
671
672
673
674
675
676
677
678
679
680
681
682
683
684
685
686
687
688
689
690
691
692
693
694
695
696
697
698
699
700
701
702
703
704
705
706
707
708
709
710
711
712
713
714
715
716
717
718
719
720
721
722
723
724
725
726
727
728
729
730
731
732
733
734
735
736
737
738
739
740
741
742
743
744
745
746
747
748
749
750
751
752
753
754
755
756
757
758
759
760
761
762
763
764
765
766
767
768
769
770
771
772
773
774
775
776
777
778
779
780
781
782
783
784
785
786
787
788
789
790
791
792
793
794
795
796
797
798
799
800
801
802
803
804
805
806
807
808
809
810
811
812
813
814
815
816
817
818
819
820
821
822
823
824
825
826
827
828
829
830
831
832
833
834
835
836
837
838
839
840
841
842
843
844
845
846
847
848
849
850
851
852
853
854
855
856
857
858
859
860
861
862
863
864
865
866
867
868
869
870
871
872
873
874
875
876
877
878
879
880
881
882
883
884
885
886
887
888
889
890
891
892
893
894
895
896
897
898
899
900
901
902
903
904
905
906
907
908
909
910
911
912
913
914
915
916
917
918
919
920
921
922
923
924
925
926
927
928
929
930
931
932
933
934
935
936
937
938
939
940
941
942
943
944
945
946
947
948
949
950
951
952
953
954
955
956
957
958
959
960
961
962
963
964
965
966
967
968
969
970
971
972
973
974
975
976
977
978
979
980
981
982
983
984
985
986
987
988
989
990
991
992
993
994
995
996
997
998
999
1000

The arching effect due to the trench sidewall friction is highly dependent on the shear strength reduction factor R , as shown in Fig. 4(c), which illustrates effective stress profiles for three cases with varied values of R (specified based on the Newcastle case modeled previously). The values of vertical effective stress for the cases with $R=0.2$, and 0.3 are 55.2% and 33.9%, respectively, of that for $R=0.1$, and those of horizontal effective stress are 60.1% and 41.2%, respectively.

A comparison between the results obtained by the numerical method which considers a linear increase of k with depth and those by the closed-form solution where the modulus of horizontal subgrade reaction k is assumed to be constant in depth is shown in Fig. 5. The k used for the closed-form solution is an average value throughout the domain of the cutoff wall (that is, $k=n_h L/2$). For the scenario in a loose sand formation, vertical effective stress is significantly underestimated by the closed-form solution, particularly in the deep region. This underestimation is because a higher sidewall friction is calculated by the closed-form solution due to greater lateral squeezing effects which result from a lower value of k being used in this region. The vertical effective stress calculated by the closed-form solution is 81.4% and 55.2% of that obtained by the numerical method at $z=15$ m and $z=30$ m, respectively. However, the closed-form solution gives a relatively

1
2
3
4 good prediction for the scenario in medium or dense sand formation, which as noted by
5
6
7 Filz (1996), is not dominated by the lateral compression mechanism.
8
9

10 11 12 13 14 **4. Conclusions** 15

16
17
18
19 A model accounting for both arching and lateral squeezing effects has been proposed to
20
21 predict the steady-state effective stresses in cutoff wall backfill. The proposed model was
22
23 then applied to a SB slurry trench cutoff wall at Mayfield, New South Wales, Australia,
24
25 and the predicted stress profile was found to be in good agreement with that calculated
26
27 from CPTu data, provided an appropriate value of shear strength reduction factor is
28
29 applied to the backfill. Compared with the stresses predicted by geostatics, the arching
30
31 model and the MLS model, the proposed method offers a significant improvement in the
32
33 prediction of stress in SB slurry trench walls. The obtained stresses can be used to
34
35 estimate the hydraulic conductivity in the backfill. It was found that the hydraulic
36
37 conductivity is relatively high in the shallow region owing to the low state of effective
38
39 stresses, which requires consideration in cutoff wall design, and decreases slightly with
40
41 the depth in the deeper regions. A parametric study found that: (1) the arching effect on
42
43 the stresses in backfill is highly dependent on the sidewall friction, and laboratory tests
44
45 on the shear strength of backfill-surrounding soil interface are required to get the value of
46
47 R ; (2) the modulus of the backfill does not have a significant impact on the effective
48
49 stresses in backfill, compared to the modulus of horizontal subgrade reaction of
50
51 surrounding soil; and (3) the closed-form solution significantly underestimates the stress
52
53
54
55
56
57
58
59
60
61
62
63
64
65

1
2
3
4 in the deep portion for the case in a loose sand formation; but it gives a relatively good
5
6 prediction for the case in medium or dense sand formation.
7
8
9

10 11 12 13 14 **Acknowledgement**

15
16
17
18
19 The financial support received from the National Natural Science Foundation of China
20
21 (NSFC) via Grant No. 51378465 and from the National High Technology Research and
22
23 Development Program of China (863 Program) via Grant No. 2012AA062601 are
24
25 gratefully acknowledged. The authors also wish to express their gratitude to Prof. Jeffrey
26
27 C. Evans, Bucknell University for providing the data of the Mayfield case history.
28
29
30
31
32
33
34
35

36 **List of Symbols**

37		
38	a	area ration of CPTu
39	c_k	change of hydraulic conductivity index
40	c'_{inter}	cohesion of backfill-surrounding soil interface
41	c'_{sb}	cohesion of SB backfill
42	k	modulus of horizontal subgrade reaction
43	k_b	hydraulic conductivity of SB backfill
44	k_{b0}	hydraulic conductivity at σ'_0
45	n	exponent to give modulus of horizontal subgrade reaction the best fit
46	n_h	constant of modulus of horizontal subgrade reaction
47	q_c	raw tip resistance of CPTu
48	q_t	corrected tip resistance of CPTu
49	u	pore water pressure
50	u_2	pore pressure read from CPTu
51	u_e	excess pore water pressure
52	y	Distance
53	z	Depth
54	A	Coefficient
55	A_s	constant of horizontal subgrade reaction
56		
57		
58		
59		
60		
61		
62		
63		
64		
65		

1		
2		
3		
4	B	width of SB slurry trench cutoff wall
5	B_s	coefficient of horizontal subgrade reaction for depth variation
6	D	Coefficient
7	E	Young's modulus of SB backfill
8	E	Young's modulus of SB backfill
9	K_{ob}	at-rest earth pressure coefficient of SB backfill
10	L	depth of SB slurry trench cutoff wall
11	N_{ke}	theoretical cone factor of CPTu
12	R	shear strength reduction factor
13	R	shear strength reduction factor
14	S_u	undrained shear strength of SB backfill
15	γ_w	unit weight of water
16	γ_w	unit weight of water
17	γ_{sb}	unit weight of SB backfill
18	γ'_{sb}	buoyant unit weight of SB backfill
19	γ'_{sb}	buoyant unit weight of SB backfill
20	μ	Poisson's ratio of SB backfill
21	σ_h	horizontal total stress in backfill
22	σ_h	horizontal total stress in backfill
23	σ'	effective consolidation stress
24	σ'_0	major principal effective stress
25	σ'_0	major principal effective stress
26	σ'_h	horizontal effective stress in backfill
27	σ'_h	horizontal effective stress in backfill
28	$\sigma'_{h,s}$	horizontal effective stress in surrounding soil
29	σ'_{mean}	mean effective stress
30	σ'_{mean}	mean effective stress
31	ϕ'_{sb}	internal friction angle of SB backfill
32	ϕ'_{sb}	internal friction angle of SB backfill
33	σ'_v	vertical effective stress in backfill
34	$\bar{\sigma}'$	equivalent vertical effective stress
35	$\bar{\sigma}'$	equivalent vertical effective stress
36	τ	sidewall frictional stress at backfill-surrounding soil interface
37	ϕ'_{inter}	internal friction angle of backfill-surrounding soil interface
38		
39		
40		
41		
42		
43		
44		
45		
46		
47		
48		
49		
50		
51		
52		
53		
54		
55		
56		
57		
58		
59		
60		
61		
62		
63		
64		
65		

1
2
3
4 **References**
5
6
7
8

9 Adams, T., Baxter, D., Boyer, R., Britton, J., Henry, L., Heslin, G., and Filz, G. (1997).
10 The Mechanical and Hydraulic Behavior of Soil-Bentonite Cutoff Walls, Progress
11 Report No. 2. Virginia Polytechnic Institute and State University, Blacksburg, VA.
12
13

14 Baxter, D. Y. (2000). *Mechanical Behavior of Soil-bentonite Cutoff Walls*. Ph.D. Thesis,
15
16 Virginia Polytechnic Institute and State University.
17
18

19 Bennert, T. A., Maher, A., and Jafari, F. (2005). Piezocone evaluation of a shallow soil-
20
21 bentonite slurry wall. *Geo-Frontiers 2005*, GSP, ASCE, 1-14.
22
23

24 Bowles, J. E. (1996). *Foundation Analysis and Design*, McGraw-Hill Companies, Inc.,
25
26 New York.
27
28

29 Das, B. M. (1998). *Principles of Foundation Engineering*, Brooks/Cole Publishing
30
31 Company, Pacific Grove, California, USA.
32
33

34 Department of Housing and Urban-Rural Development of Zhejiang Province
35
36 (DHURDZP) (2014). Technical Specification for Building Foundation Excavation
37
38 Engineering. Zhejiang Gongshan University Press, Hangzhou.
39
40

41 Evans, J. C. (1994). Hydraulic conductivity of vertical cutoff walls evans. *Hydraulic*
42
43 *Conductivity and Waste Containment Transport in Soil*, ASTM, Philadelphia, 79-94.
44
45

46 Evans, J. C., Costa, M. J., and Cooley, B. (1995). The state-of-stress in soil-bentonite
47
48 slurry trench cutoff walls. *Geoenvironment 2000: Characterization, Containment,*
49
50 *Remediation, and Performance in Environmental Geotechnics*, ASCE,
51
52 Geotechnical Specialty Publication, New York, NY, 1173-1191.
53
54
55
56
57
58
59
60
61
62
63
64
65

- 1
2
3
4 Filz, G. M. (1996). Consolidation stresses in soil-bentonite backfilled trenches. *The 2nd*
5
6
7 *International Congress on Environmental Geotechnics*, Balkema, Rotterdam, 497-
8
9 502.
- 10
11 Filz, G. M., Henry, L. B., Heslin, G. M., and Davidson, R. R. (2001). Determining
12
13 hydraulic conductivity of soil-bentonite using the API filter press. *Geotechnical*
14
15 *Testing Journal*, 24, No. 1, 61-71.
- 16
17
18
19 Fox, P. J., Pu, H. F., and Berles, J. D. (2014). CS3: Large Strain Consolidation Model for
20
21 Layered Soils. *Journal of Geotechnical and Geoenvironmental Engineering*, 140,
22
23 No. 8, 04014041-1-13.
- 24
25
26 Handy, R. L. (1985). The arch in soil arching. *Journal of Geotechnical Engineering-*
27
28 *ASCE*, 111, No. 3, 302-318.
- 29
30
31 Jones, S., Spaulding, C., and Symth, P. (2007). Design and construction of a deep soil-
32
33 bentonite groundwater barrier wall at Newcastle, Australia. *10th Australian New*
34
35 *Zealand Conference on Geomechanics Common Ground*.
- 36
37
38 Lam, C., Jefferis, S. A., and Martin, C. M. (2014). Effects of polymer and bentonite
39
40 support fluids on concrete-sand interface shear strength. *Géotechnique*, 64, No. 1,
41
42 28-39.
- 43
44
45 McCandless, R., and Bodocsi, A. (1987). Investigation of slurry cutoff wall design and
46
47 construction methods for containing hazardous wastes. U.S. Environmental
48
49 Protection Agency, Washington, D.C.
- 50
51
52
53 National Research Council (2007). *Assessment of the performance of engineered waste*
54
55 *containment barriers*, National Academies Press, Washington, D.C.
- 56
57
58
59
60
61
62
63
64
65

- 1
2
3
4 Potyondy, J. G. (1961). Skin friction between various soils and construction materials
5
6 *Géotechnique*, 11, No. 4, 339-353
7
8
9 Powell, J., and Lunne, T. (2005). Use of CPT data in clays/fine grained soils. *Studia*
10
11 *Geotechnica et Mechanica*, 27, No. 3-4, 53-63.
12
13
14 Ruffing, D. G., Evans, J. C., and Malusis, M. A. (2010). Prediction of earth pressures in
15
16 soil-bentonite cutoff walls. *GeoFlorida*, 2416-2425.
17
18
19 Ruffing, D. G., Evans, J. C., and Malusis, M. A. (2012). Long term in situ measurements
20
21 of the volumetric water content in a soil-bentonite slurry trench cutoff wall.
22
23 *GeoCongress 2012: State of the Art and Practice in Geotechnical Engineering*,
24
25 3429-3436.
26
27
28 Ruffing, D. G., Evans, J. C., and Ryan, C. R. Strength and stress estimation in soil
29
30 bentonite slurry trench cutoff walls using cone penetration test data. *Proc.*,
31
32 *Proceedings of The International Foundations Congress and Equipment Expo 2015*.
33
34
35
36 Ryan, C. R., and Spaulding, C. A. (2008). Strength and permeability of a deep soil
37
38 bentonite slurry wall. *GeoCongress 2008: Geotechnics of Waste Management and*
39
40 *Remediation*, ASCE, 644-651.
41
42
43 Selvadurai, A. P. S. (1979). *Elastic Analysis of Soil-Foundation Interaction*, Elsevier
44
45 Scientific Pub. Co., New York.
46
47
48 Timoshenko, S. (1970). *Theory of Elasticity*, McGraw-Hill Publishing Company, New
49
50 York.
51
52
53 Yeo, S. S., Shackelford, C. D., and Evans, J. C. (2005). Consolidation and hydraulic
54
55 conductivity of nine model soil-bentonite backfills. *Journal of Geotechnical and*
56
57 *Geoenvironmental Engineering*, ASCE, 131, No. 10, 1189-1198.
58
59
60
61
62
63
64
65

1
2
3
4
5
6
7
8
9
10
11
12
13
14
15
16
17
18
19
20
21
22
23
24
25
26
27
28
29
30
31
32
33
34
35
36
37
38
39
40
41
42
43
44
45
46
47
48
49
50
51
52
53
54
55
56
57
58
59
60
61
62
63
64
65

List of Table and Figure Captions

Table 1. Pore pressure and horizontal stress in SB backfill at depth of z .

Table 2. Geometric and material properties for Mayfield site analysis.

Table 3. Geometric and material properties in parametric study.

Fig. 1. Diagram of a SB cutoff wall in Winkler foundation (not in scale).

Fig. 2. Predicted effective stress in soil-bentonite slurry trench cutoff wall of Mayfield site.

Fig. 3. Estimated hydraulic conductivity profiles based on effective stresses for soil-bentonite slurry trench cutoff wall of Mayfield site.

Fig. 4. Stress profiles obtained in parametric study.

Fig. 5. Stress profiles for varied functions of the modulus of horizontal subgrade reaction of surrounding soil.

Table 1. Pore water pressure and stress in SB backfill at depth of z .

Pore water pressure or stress in backfill at depth of z	Corresponding time	
	Backfill is placed	Backfill is consolidated
u_e	$\gamma'_{sb} z$	0
u	$\gamma_{sb} z$	$\gamma_w z$
σ'_h	0	to be determined
σ'_v	0	to be determined
σ_h	$\gamma_{sb} z$	$\gamma_w z + \sigma'_h$

Table 2. Geometric and material properties for Mayfield site analysis.

Parameter	Value	Unit
B	0.8*	m
γ'_{sb}	9.3 [#]	kN/m ³
E	654 [†]	kPa
μ	0.35	/
c'_{sb}	0.0 [†]	kPa
ϕ'_{sb}	30.0 [†]	°
n_h	7.7	MN/m ⁴
R	0.12	/

*: Jones et al. (2007); #: Ryan & Spaulding (2008); †: Ruffing et al. (2010).

Table 3. Geometric and material properties in parametric study.

Parameter	Value	Unit
B	0.6	m
L	30.0	m
γ'_{sb}	9.7*	kN/m ³
E	654 (312, 997)*	kPa
μ	0.35	/
c'_{sb}	0.0*	kPa
ϕ'_{sb}	30.0*	°
n_h	4.8 (1.2, 10.6) [#]	MN/m ⁴
R	0.12 (0.1, 0.2, 0.3)	/

*: from Ruffing et al. (2010); #: from Das (1998).

Figure 1

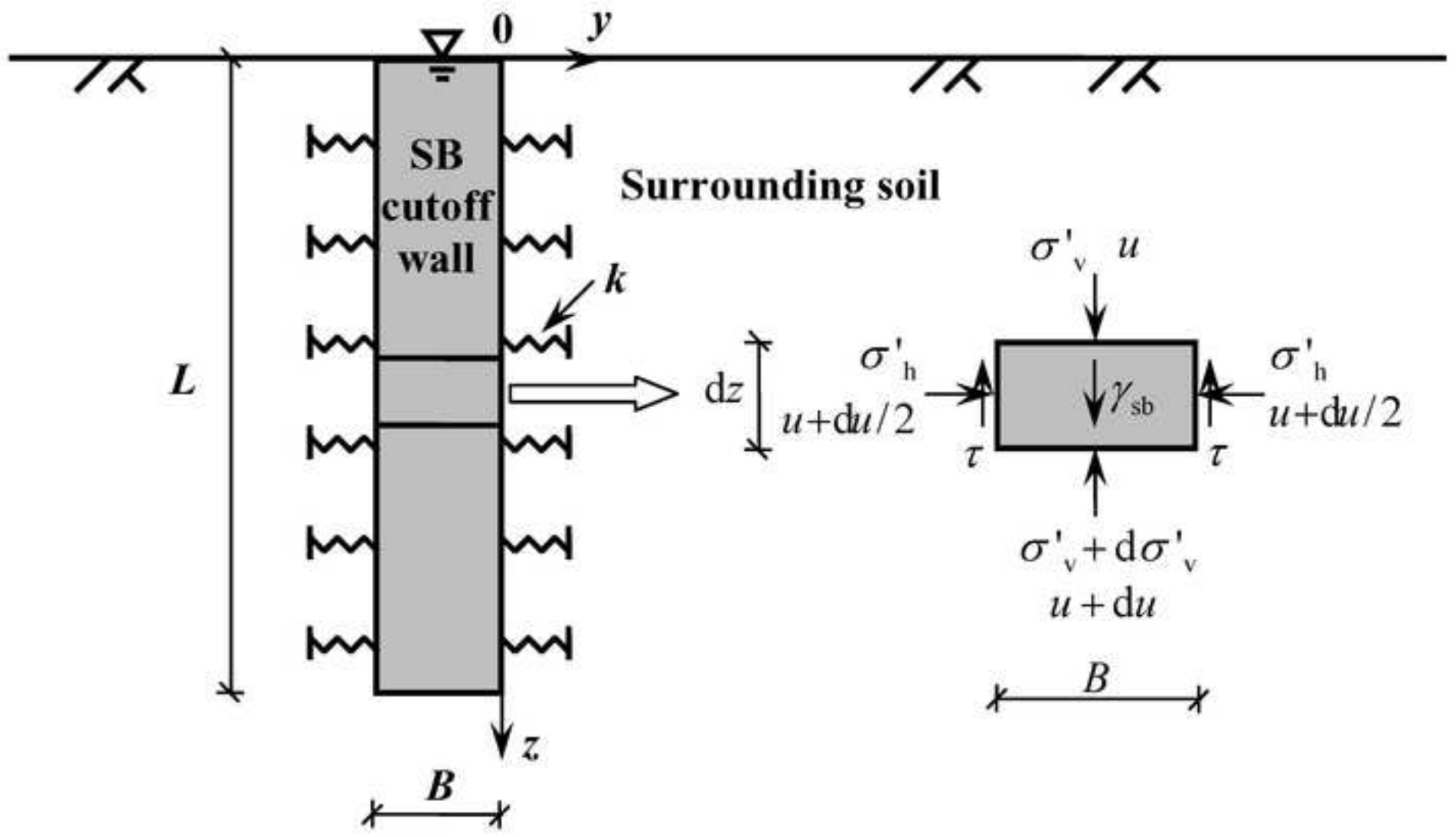


Figure 2

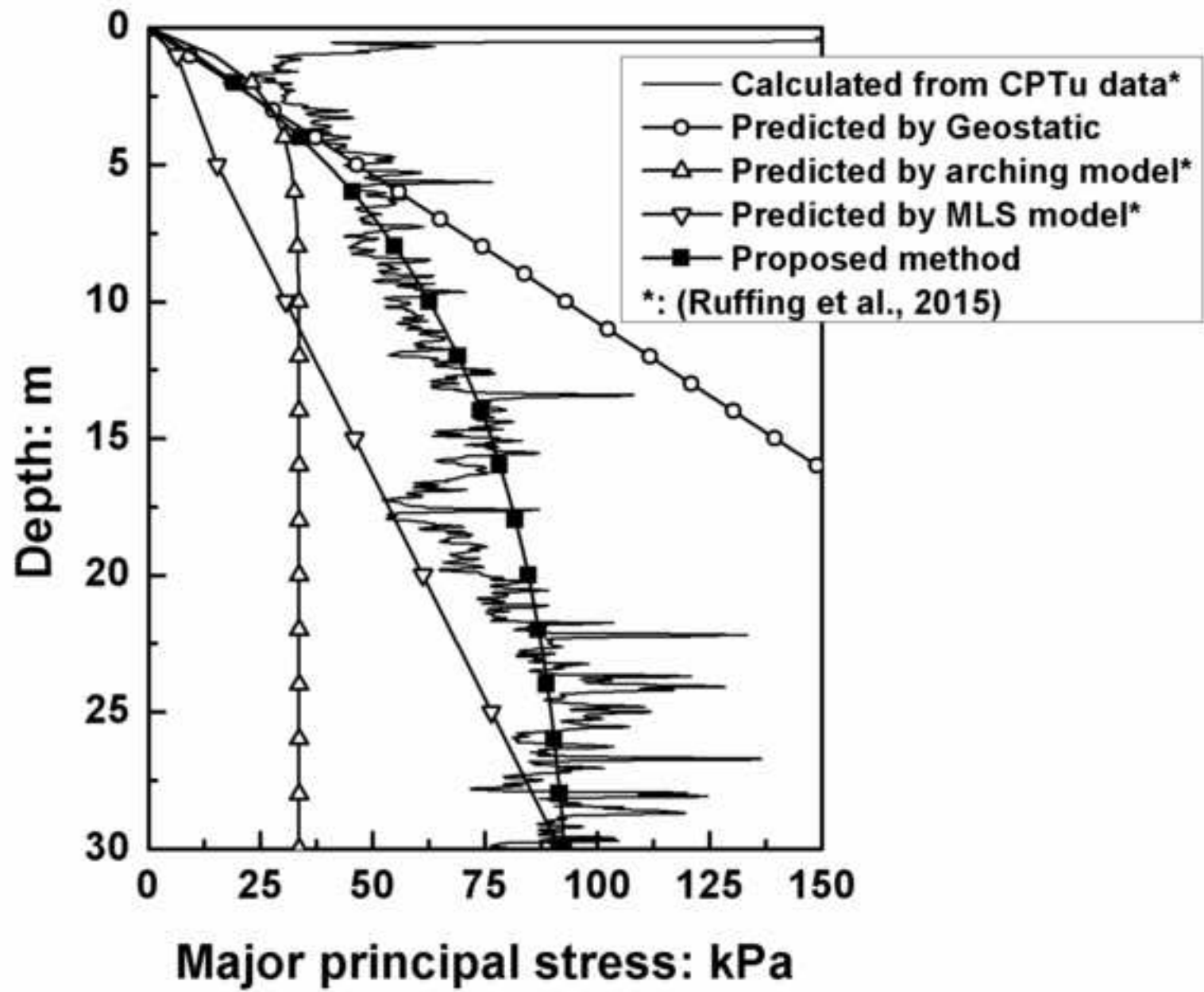


Figure 3

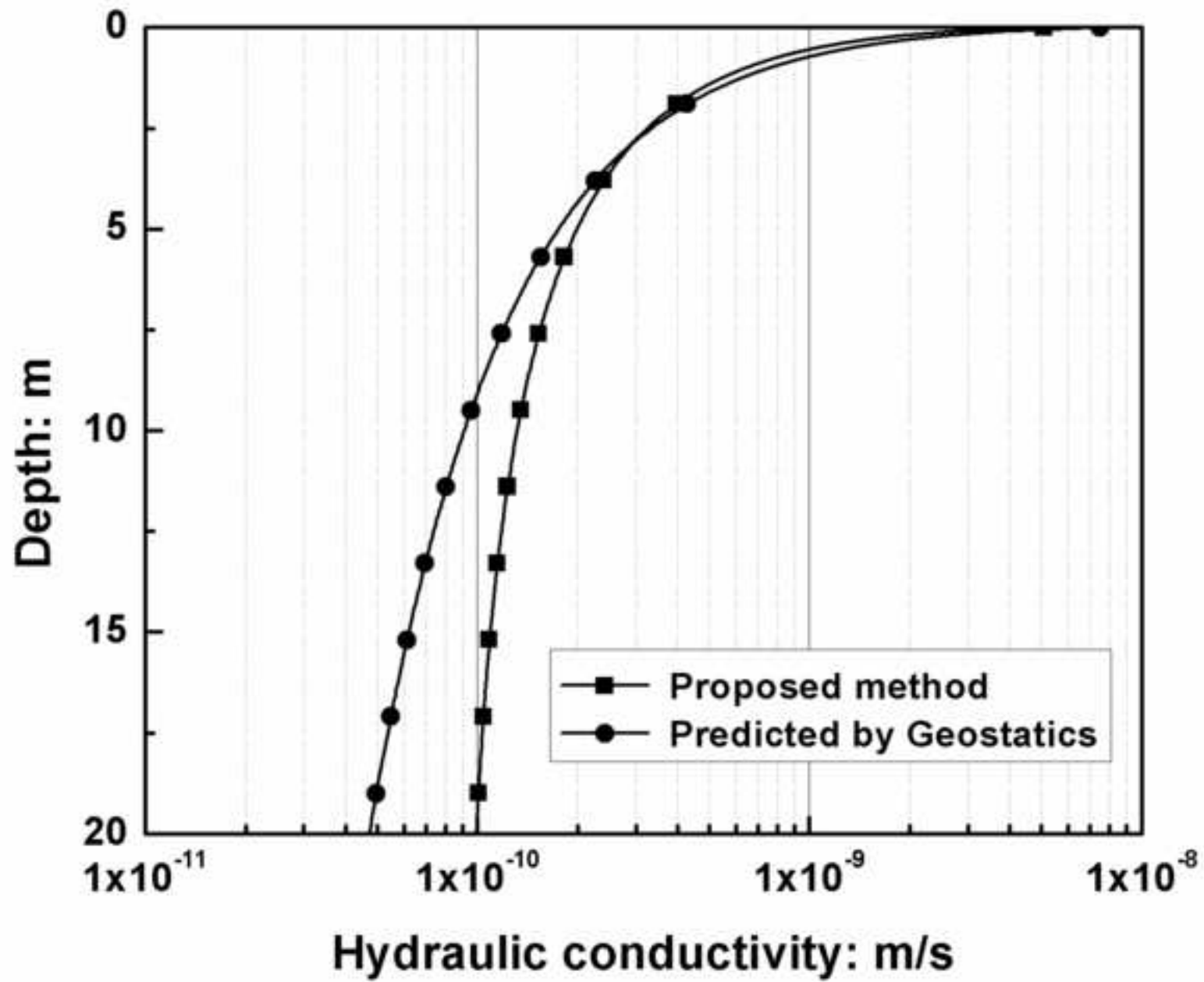


Figure 4(a)

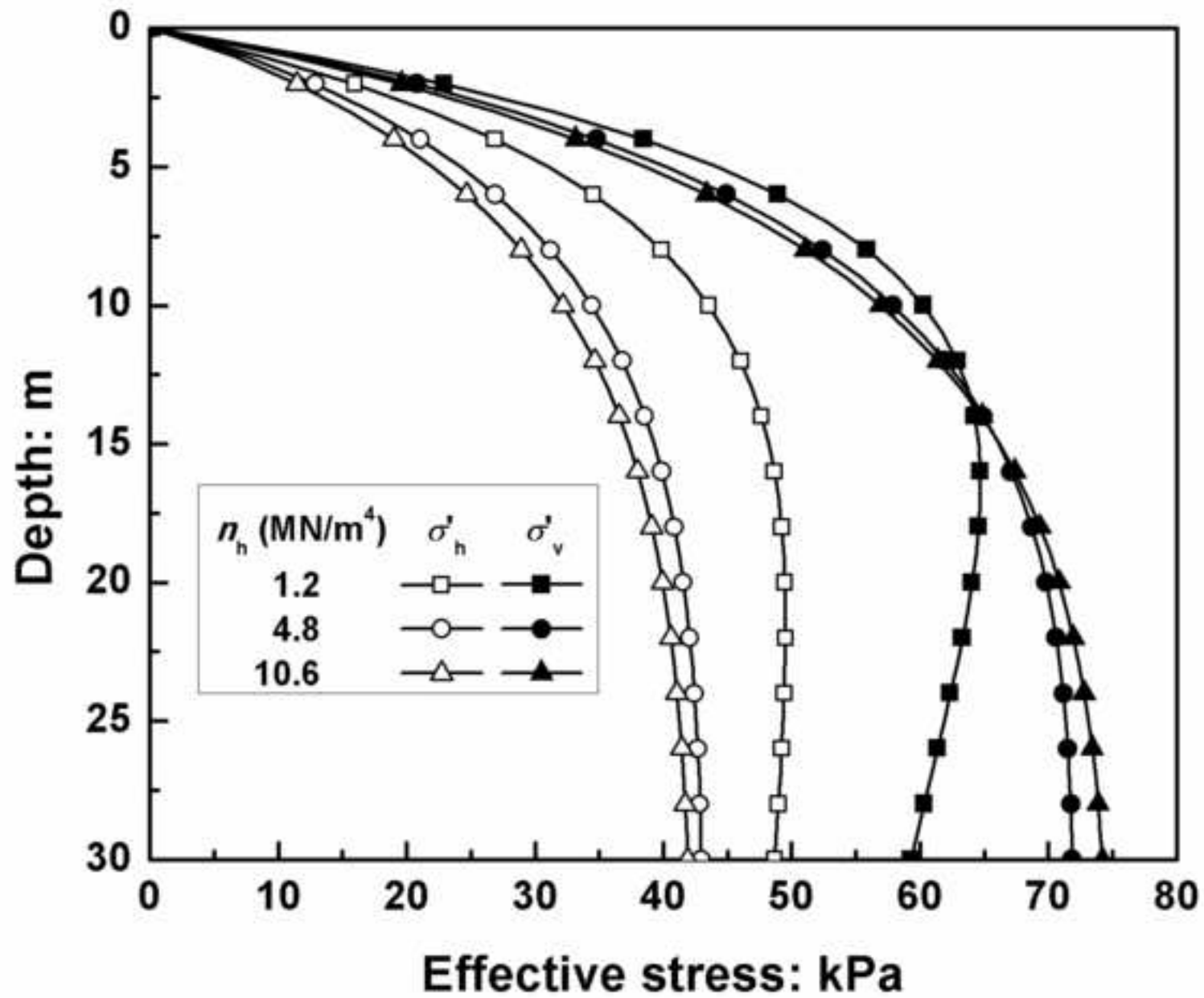


Figure 4(b)

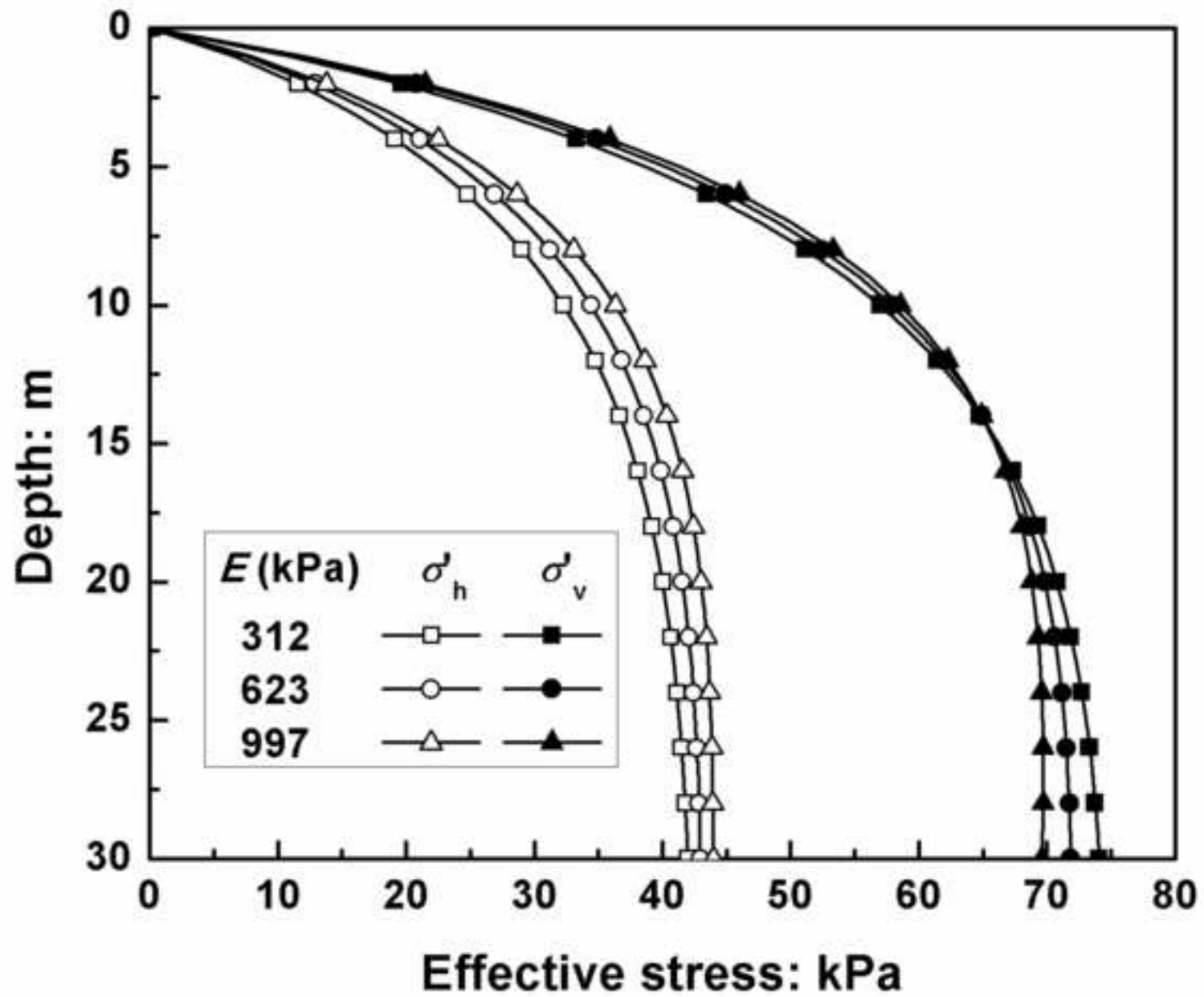


Figure 4(c)

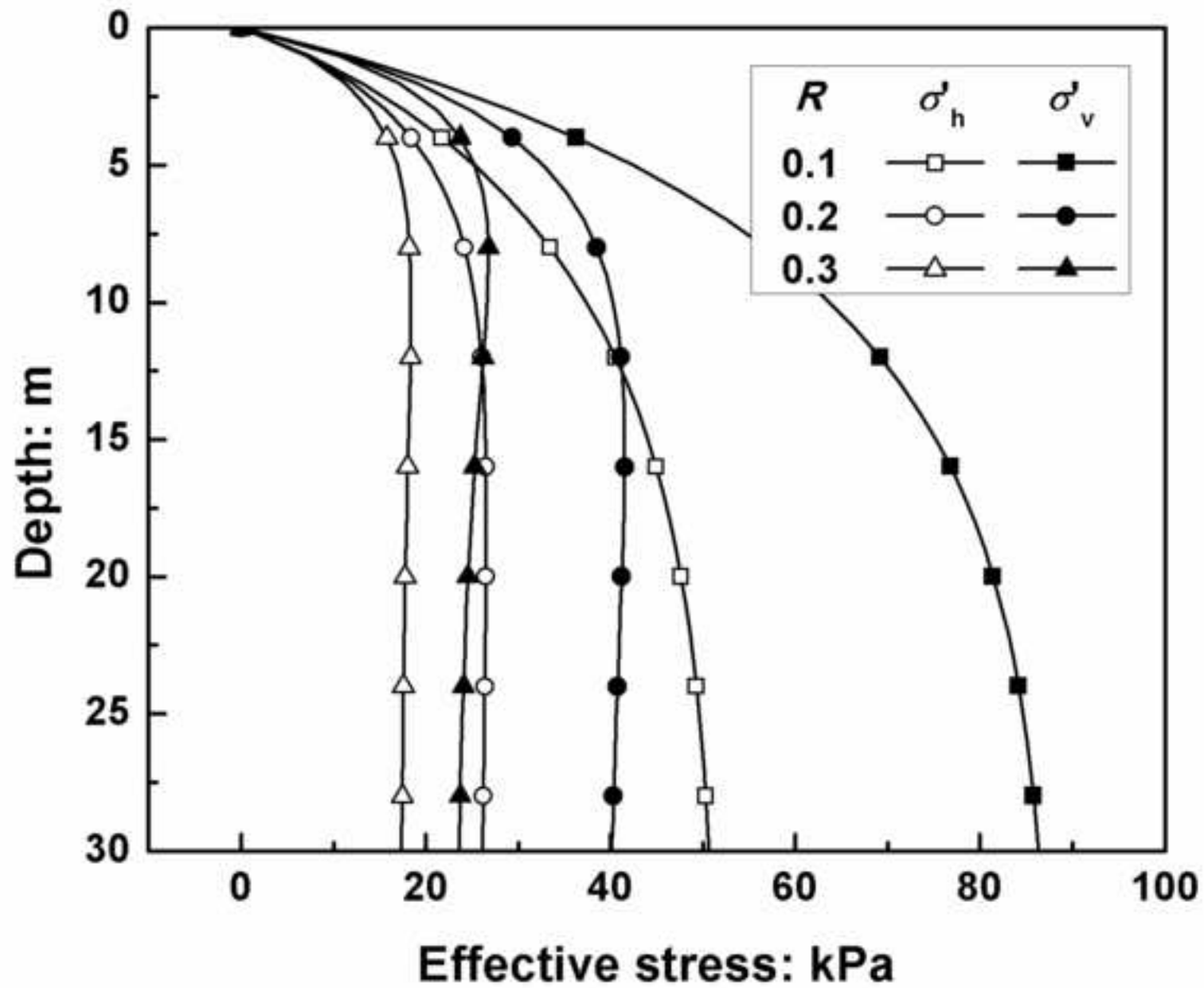


Figure 5

